CME Article

Cardiac autonomic imaging with SPECT tracers

Mark I. Travin, MD

Radionuclide cardiac imaging has potential to assess underlying molecular, electrophysiologic, and pathophysiologic processes of cardiac disease. An area of current interest is cardiac autonomic innervation imaging with a radiotracer such as ^{123}I-*meta*-iodobenzylguanidine (^{123}I-*m*IBG), a norepinephrine analogue. Cardiac ^{123}I-*m*IBG uptake can be assessed by planar and SPECT techniques, involving determination of global uptake by a heart-to-mediastinal ratio, tracer washout between early and delayed images, and focal defects on tomographic images. Cardiac ^{123}I-*m*IBG findings have consistently been shown to correlate strongly with heart failure severity, pre-disposition to cardiac arrhythmias, and poor prognosis independent of conventional clinical, laboratory, and image parameters. ^{123}I-*m*IBG imaging promises to help monitor a patient's clinical course and response to therapy, showing potential to help select patients for an ICD and other advanced therapies better than current methods. Autonomic imaging also appears to help diagnose ischemic heart disease and identify higher risk, as well as risk-stratify patients with diabetes. Although more investigations in larger populations are needed to strengthen prior findings and influence modifications of clinical guidelines, cardiac ^{123}I-*m*IBG imaging shows promise as an emerging technique for recognizing and following potentially life-threatening conditions, as well as improving our understanding of the pathophysiology of various diseases.

Key Words: MIBG imaging • iodine-123 • molecular imaging • autonomic imaging

INTRODUCTION

Radionuclide cardiac imaging, i.e., nuclear cardiology, is a well-established noninvasive method of evaluating patients with known or suspected heart disease. Its focus has been mainly on assessment of coronary artery disease (CAD) using myocardial perfusion imaging (MPI), enhanced by methods that evaluate left ventricular (LV) function and myocardial viability. The clinical utility of MPI has been well described and is broadly accepted.[1-11]

Nevertheless, heart disease encompasses more than CAD, and nuclear cardiology has much to offer beyond MPI. In particular, radionuclide imaging can assess molecular processes, helping to better understand the underlying cardiac pathophysiology, and thereby improving our ability to manage patients.[12-14] A method under active investigation is imaging of the cardiac autonomic system that plays a major role in maintaining hemodynamic and electrophysiological stability at rest and in response to changing demands. In the setting of disease, autonomic control is often disrupted, with resultant image abnormalities that are both a reflection of disease severity and a prediction of further clinical deterioration.[15] There is accumulating evidence that imaging with autonomic radiotracers can evaluate patients with a wide variety of cardiac conditions, including heart failure (HF), arrhythmias, and ischemic heart disease, providing highly effective risk stratification and therefore a potential guide for improving patient management.

CARDIAC AUTONOMIC ANATOMY AND PHYSIOLOGY

Cardiac autonomic control consists of both local innervation and circulating chemicals, and consists of the sympathetic and parasympathetic systems.[16-18] The neurotransmitter of the sympathetic system is

From the Division of Nuclear Medicine, Department of Radiology, Montefiore Medical Center, Albert Einstein College of Medicine, Bronx, NY.

Reprint requests: Mark I. Travin, MD, Division of Nuclear Medicine, Department of Radiology, Montefiore Medical Center, Albert Einstein College of Medicine, 111 East-210th Street, Bronx, NY 10467-2490; *mtravin@montefiore.org*.

J Nucl Cardiol 2013;20:128–43.
1071-3581/$34.00

doi:10.1007/s12350-012-9655-1

norepinephrine (NE), and that of the parasympathetic system is acetylcholine (ACh), working together to stimulate or inhibit the heart via adrenergic and muscarinic receptors. Sympathetic output is regulated by centers in the brain that integrate signals from other parts of the brain and receptors throughout the body (e.g., carotid sinus, aortic arch, origin of right subclavian artery, intracardiac). Efferent signals follow descending pathways in the spinal cord, synapsing with pre-ganglionic fibers and then paravertebral stellate ganglia, eventually innervating the right ventricle, and the anterior and lateral LV. In the heart, sympathetic nerves follow the coronary arteries in the subepicardium, before penetrating into the myocardium.

Parasympathetic fibers are relatively scarce. They begin in the medulla and follow the vagus nerves. They start epicardially in the heart, cross the atrioventricular (AV) groove, and penetrate the myocardium to be located in the subendocardium. Parasympathetic fibers predominantly innervate the atria, and are scarce in the ventricle (mostly the inferior wall), and also modulate sinoatrial (SA) and atrioventricular (AV) nodal function.

Published literature and clinical experience predominantly involve the sympathetic system, with parasympathetic imaging work reported mostly in animals. This review will therefore be limited to the former.

DEVELOPMENT OF AUTONOMIC RADIOTRACERS

Most autonomic radiotracers under investigation image pre-synaptic anatomy and function, illustrated in Figure 1[19,20] (although there is ongoing work on PET tracers that bind to post-synaptic α and β receptors). NE is produced in the pre-synaptic terminal, and is concentrated and stored in vesicles, often with ATP. In response to a stimulus, vesicular contents are released into the synaptic space and bind to postsynaptic receptors, resulting in cardiac stimulatory effects.[21,22]

Control of the sympathetic response occurs through a transporter protein-mediated, sodium-, and energy-dependent process, known as ''uptake-1,' (or norepinephrine transporter 1, i.e., NET-1) for storage and/or catabolic disposal, thereby terminating the stimulus. Some free NE is also taken up by non-neuronal postsynaptic cells, probably by sodium-independent passive diffusion (i.e., ''uptake-2'').[23,24]

The development of autonomic radiotracers is well chronicled in a recent review by Raffel and Wieland. Cardiac tracer development was the unintended result of efforts by Dr William H. Beierwaltes, then Chief of Nuclear Medicine at the University of Michigan, to develop scintigraphic imaging for adrenal diseases, particularly neoplasms associated with the medulla.[25] There

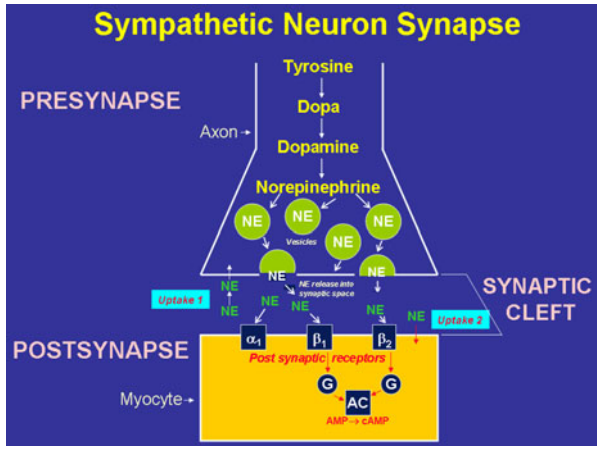

Figure 1. Schematic representation of the sympathetic neuron synapse. *AC*, Adenyl cyclase; *AMP*, adenosine monophosphate; *cAMP*, cyclic adenosine monophosphate; *G*, G proteins; *NE*, norepinephrine. Reprinted from Cardiology Clinics: Nuclear Cardiology—From Perfusion to Tissue Biology, Vol. 27, Travin[19] Copyright 2009, with permission from Elsevier.

researchers explored using iodine (I)-labeled analogues of the adrenergic blocking antiarrhythmic drug bretylium to image myocardial infarcts, finding that a *para*-iodobretylium analog also effectively imaged the canine adrenal medulla.[26,27] The work continued with newly recruited radiochemist, Don Wieland, PhD, who investigated a related compound, guanethidine, a false neurotransmitter analog of NE. In 1979, it was determined that iodine in the *meta*-position yielded a tracer with comparable uptake to having iodine in the *para*-position but was metabolically more stable, and thus *meta*-iodobenzylguanidine, i.e., *m*IBG was selected as the optimal agent for adrenomedullary imaging.[28] Cardiac *m*IBG uptake was also strong, with a significantly higher heart-to-blood uptake than the perfusion tracer then under investigation, ^{201}Thallium (Tl). As per observations of Wieland, in contrast to thallium that depicted the ''plumbing'' of the heart, *m*IBG imaging allowed visualization of the ''wiring'' of the heart. The first publication of human heart imaging was in 1981 by Kline et al.,[29] and shortly thereafter *m*IBG imaging was speculated as having the potential to assess the pathophysiology of HF, and identify patients with autonomic neuropathies who may be predisposed to arrhythmias and sudden cardiac death (SCD).[30-32] Masyuki Nakajo MD, a visiting fellow from Japan, observed an inverse correlation between cardiac *m*IBG uptake, and plasma and urinary catecholamine levels,[33] and after returning to Japan found that intraneuronal uptake of the tracer into storage vesicles was a key process.[34] Shortly thereafter, efforts at Michigan shifted toward positron emission tomography (PET) compounds, resulting in clinical *m*IBG studies thereafter being performed mostly in Europe and Japan.

While early in development, *m*IBG was labeled with ^{131}I, high energy emissions (365 keV), including β^- particles, and the 8-day half-life led to use of ^{123}I that emits predominantly 159-keV gamma photons, with a half-life of 13.2 h, thus well-tolerated and easily imaged with single-photon emission computed tomography (SPECT). Unlike NE, after uptake in the pre-synaptic terminal via the NET-1 pathway, ^{123}I-*m*IBG is not catabolized, and thereby localizes to a high cytoplasmic concentration.[29,35]

IMAGING PROCEDURE AND INTERPRETATION

Cardiac imaging with ^{123}I-*m*IBG has been used clinically in Europe and Japan for years, but at the time of this writing is only US FDA approved to image pheochromocytomas and neuroblastomas (under the brand name AdreView™). There is no established standard for tracer administration and imaging. Flotats et al,[36] with the European Association of Nuclear Medicine and the European Council of Nuclear Cardiology, recently proposed such a standard.

Tracer Administration

^{123}I-*m*IBG is performed at rest with only minimal preparation. Standards for a recent multicenter study were to keep the patient NPO.[37] Based on several studies it is accepted that standard HF medications such as β-blockers, angiotensin-converting enzyme inhibitors (ACE-I), and/or angiotensin receptor blockers (ARBs) need not be held.[38-40] However, it is recommended to temporarily discontinue medications and substances known to interfere directly with the mechanism of NE uptake, such as opioids and cocaine, tricyclic antidepressants, sympathicomimetics (e.g., ephedrine, pseudoephedrine, phenylephrine, isoproterenol), some antihypertensive and cardiovascular agents (e.g., labetolol, reserpine, bretylium, calcium channel blockers), antipsychotics (e.g., phenothiazines), and foods containing vanillin and catecholamine-like compounds (e.g., chocolate and blue cheese).[41,42]

There are differing views regarding pre-test administration of thyroid blocking agents. Historically such blockade had been undertaken to shield the thyroid from exposure to unbound radionuclide iodine impurities, but with modern production methods the amount of these is minimal, and many feel that pre-treatment is unnecessary. For now, pre-treatment should be based on local and institutional regulations.[37]

Earlier studies administered a dose of 3-5 millicuries (mCi) (111-185 megabecquerels (MBq)) over 1 minute. As it is often difficult to obtain satisfactory SPECT images using these doses, especially in patients with severe cardiac dysfunction, investigators have recently been using up to 10 mCi (370 MBq).[22,37]

It has been recommended that patients lie quietly in a supine position for at least 5 minutes before administration. As initial images are acquired a few minutes later, the tracer is best administered slowly over 1-2 minutes while the patient is under the camera or in close proximity.

Adverse reactions to ^{123}I-*m*IBG are uncommon. Among side effects reported when administered too quickly are palpitations, shortness of breath, heat sensations, transient hypertension, and abdominal cramps. A rare anaphylactic reaction is also possible. A 10 mCi dose results in radiation exposure of ~5 mSv, with highest exposure to the bladder, liver, spleen, gall bladder, heart, and adrenals; the absorbed dose may be higher in patients with severe renal impairment.[36]

Imaging Technique

^{123}I-*m*IBG is currently imaged using a standard Anger gamma camera, with a symmetrically centered energy window of 20% around the main 159-keV isotope photopeak. Most clinical and published work use a low energy high-resolution (LEHR) collimator, although slight differences among collimators in different countries (US vs Europe vs Japan) yield slightly different normal quantitative values. However, because of septal penetration by higher energy (>400 keV) ^{123}I photons, mostly a 529-keV emission, some have recommended using a medium energy collimator that has been shown to provide superior quantitative accuracy.[36,43,44] To compensate for the resulting corruption of image quantitation related to LEHR collimator penetration by higher energy photons, Chen et al[45,46] have developed a mathematical technique (iterative reconstruction with deconvolution of septal penetration) that appears to improve quantitative accuracy of cardiac ^{123}I-*m*IBG uptake in reference to a phantom standard. Clinical applications have yet to be determined.

Much data about ^{123}I-*m*IBG imaging is based on analysis of planar images, mostly a standard anterior view. Planar images are typically acquired 15-20 minutes after tracer injection (early image) with the patient supine, and again 4 hours later (late image), for 10 minutes each. SPECT images can also be acquired using standard perfusion imaging methods.[36] Eventually other acquisition, processing, and display techniques may be developed given issues such as often extremely poor cardiac uptake in patients with advanced HF, frequent uptake in adjacent lung and liver that overlap myocardial walls, and the need in many cases for absolute as opposed to relative quantitative myocardial tracer uptake.

As interpretation of planar images requires analysis of the upper mediastinum, there is concern that smaller field of view cardiac cameras, or performing SPECT imaging alone, would not be suitable for cardiac ^{123}I-*m*IBG imaging. However, a recent study by Chen et al.[47] reported development of a technique to derive satisfactory quantitative parameters for SPECT imaging limited to the cardiac field

Image Analysis and Interpretation

Analysis of cardiac ^{123}I-*m*IBG images consists of quantitative analysis of global uptake, i.e., the heart-to-mediastinal ratio (H/M); the difference in tracer uptake/retention in early and late images, i.e., the washout rate (WR); and regional uptake on SPECT images, often in relation to uptake in separately obtained standard perfusion images. Methods for all analyses remain under investigation.

At least three methods have been described to obtain an H/M ratio. In one, squares or rectangular regions of interest (ROIs) are drawn in the center of the heart and upper mediastinum, with a count per pixel ratio calculated.[48] In another, an ROI is drawn around the epicardial border and the valve plane, including the LV cavity.[49] Finally, some use an ROI encompassing the myocardium alone, tracing the epicardial and endocardial borders, excluding the valve plane and cavity.[50] Interestingly, all methods appear to give similar result. Figure 2 illustrates a method recommended in the European guidelines,[36] with counts/pixel in the myocardial ROI divided by count/pixel in a mediastinal box located above the lung apices, below the thyroid gland. Techniques are being explored to standardize the H/M ratio, with Okuda et al[51] describing an algorithm that automatically determines the mediastinal ROI based on tracer uptake in the heart, lung, liver, and thyroid. Normal values for H/M range from 1.9 to 2.8, a mean of 2.2 ± 0.3, with a ratio <1.6 (2 SD below mean) investigated as indicative of possible increased patient risk.[35,37] Figure 3 shows examples of normal and abnormal global cardiac ^{123}I-*m*IBG uptake.

^{123}I-*m*IBG washout, i.e., the difference in cardiac activity between early and late planar images (compensated for radioactive decay), may reflect turnover of catecholamines attributable to sympathetic drive, and measures the ability of myocardium to retain tracer. The level of circulating catecholamines may also affect washout.[52] A normal value has been reported to be 10% ± 9%.[53,54] Increased sympathetic activity, reflecting worsened HF, is associated with diminished myocardial ^{123}I-*m*IBG retention on delayed images and thus a higher myocardial WR.[55] Although various methods of washout determination are reported, recent European guidelines indicate the following[36]:

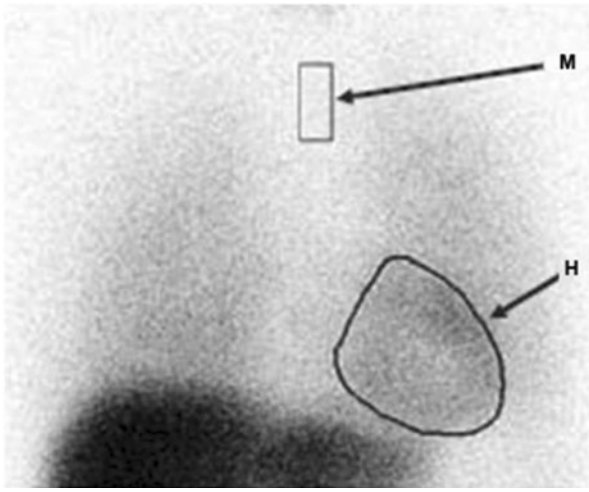

Figure 2. Method of H/M ratio determination. Counts per pixel in the myocardial heart (H) region of interest are divided by those in the mediastinum (M). Reprinted from Flotats[12,36] with kind permission from Springer Science and Business Media.

$$\mathrm{WR}_{\mathrm{BKGcorrected}} = \frac{\{H_e - M_e\} - \{(H_l - M_l) \times 1.21\}}{(H_e - M_e)} \times 100,$$

with 1.21 the correction for ^{123}I decay at 3 hours and 45 minutes, e the early images, l the late images, BKG the background, *H* the heart counts per pixel, *M* the mediastinal counts per pixel, and WR the washout rate.

Interpretation of tomographic ^{123}I-*m*IBG images is less well established, in part because of frequent poor quality, as well as variations in normal individuals. The rationale for SPECT is that the presence of regional autonomic tracer defects, particularly if tracer uptake is relatively preserved on a separately obtained standard rest perfusion image, i.e., an autonomic/perfusion mismatch, may indicate potential for electrical heterogeneity and denervation supersensitivity, pre-disposing to potentially lethal arrhythmias.[56,57]

While there is no officially established method for scoring SPECT ^{123}I-*m*IBG images, analysis can be performed similar to the conventional 17-segment method used for MPI, with generation of a summed score.[37,58] However, a key difference for ^{123}I-*m*IBG images is that when there is globally decreased uptake, homogeneous tracer uptake cannot be scored as normal as, unlike the custom for perfusion images, one cannot assume a ''normal'' region.[59] A software program that incorporates the issue of globally decreased uptake has been developed and is being tested for the Emory Cardiac Toolbox application (personal communication Ernest V. Garcia, PhD, and Russell D. Folks, CNMT). Another problem relates to frequent overlying

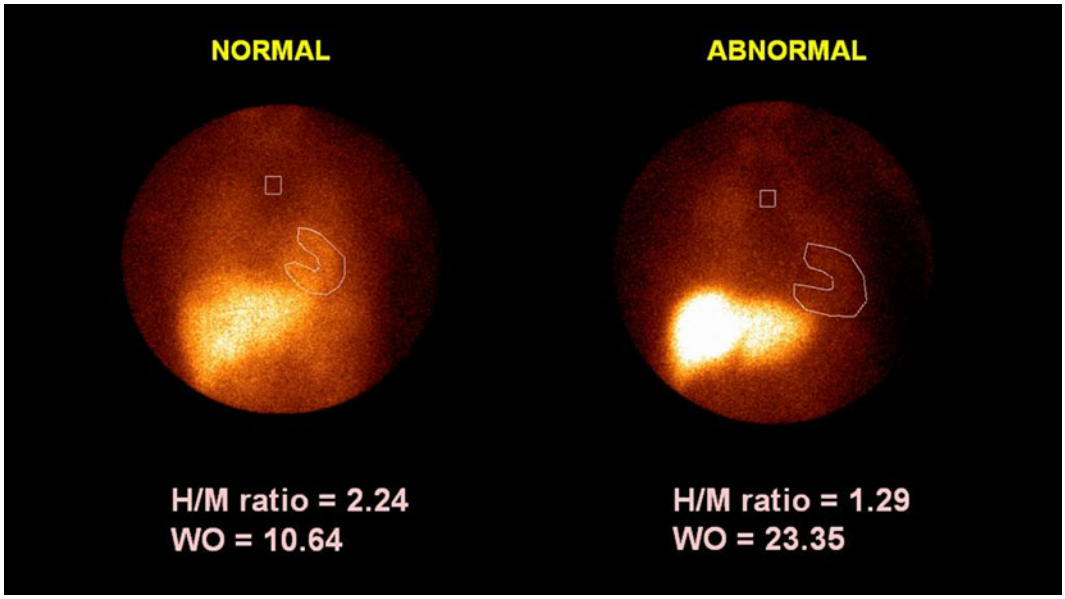

Figure 3. Examples of planar cardiac ^{123}I-*m*IBG images. The example on the *left* shows normal cardiac ^{123}I-*m*IBG uptake with a H/M ratio of 2.24 and a normal tracer washout (WO) rate from initial to delayed images (not shown) of 10.64%. The example on the *right* shows abnormal cardiac 123I-mIBG uptake with a H/M ratio of 1.29 in images and an abnormal tracer washout of 23.35%. Reprinted from Ji and Travin[20] with kind permission from Springer Science and Business Media.

extracardiac (lung and liver) activity that can obscure parts of the myocardium.

Regional ^{123}I-*m*IBG uptake can be heterogeneous in healthy individuals. Somsen et al[54] observed lower activity in the inferior than the lateral wall possibly from anatomic variation in sympathetic nerve activity. Heterogeneities may be more pronounced in men and healthy older subjects.[60] Estorch et al[61] found ^{123}I-*m*IBG uptake to be lower in the inferior wall in athletes with sinus bradycardia, perhaps from increased vagal tone. Positron emission tomographic (PET) tracers such as ^{11}C-hydroxyephedrine (HED) and ^{11}C-epinephrine also show normal heterogeneity, but less so, suggesting that there are both physiologic and technical issues involved.[62]

CLINICAL APPLICATIONS

Heart Failure

The most investigated clinical use of cardiac ^{123}I-*m*IBG imaging is in patients with HF, a condition of high morbidity and mortality affecting >6 million American over age 20.[63] As HF largely involves disruption of the neurohormonal state, including activation of the renin-angiotensin-aldosterone system (RAAS) and compensatory activation of the sympathetic nervous system (SNS), cardiac neuronal innervation is thought to play a key pathophysiologic role.[64] An increased sympathetic response in HF patients with reduced cardiac output leads to deleterious neurohormonal and myocardial structural changes that worsen the condition and increase the likelihood of a poor outcome. Initially a compensatory attempt to maintain cardiac output leads to increased NE release, promoting the NE transporter 1 (NET-1) process. Eventually the NET-1 system is overwhelmed, with a reduction in NET-1 carrier density, leading to increased spillover of NE into plasma, likely accounting for the increased washout seen on ^{123}I-*m*IBG imaging in patients with HF. With progression of cardiac dysfunction there is diminished pre-synaptic function from loss of neurons and down-regulation of NET-1, likely accounting for decreased cardiac uptake (lower H/M) in advanced disease.[52]

Following the initial report by Kline et al of human cardiac ^{123}I-*m*IBG imaging, Schofer et al[65] were the first to describe a potential role for ^{123}I-*m*IBG imaging in HF, finding decreased cardiac uptake in 28 patients with idiopathic dilated cardiomyopathy that correlated inversely with LVEF, but surprisingly did not relate to circulating catecholamine. Prognostic utility was first reported in a 1992 landmark study by Merlet et al of 90 patients with advanced HF (NY Heart Association (NYHA) Class II-III symptoms and LVEF <45%), finding that H/M was superior to and independent of cardiac size on chest x-ray, echocardiographic end-diastolic diameter, and LVEF in predicting survival.[66] An H/M < 1.2 was associated with 6- and 12-month

survivals of 60% and 40%, respectively, while all patients with H/M $\geq$ 1.2 survived despite severe HF.

Subsequent work by Nakata et al[67] of 400 patients showed the utility of H/M as a continuous variable, with progressively worsening survival as the H/M decreased, with H/M again a more powerful predictor of outcome than other conventional HF variables such as NYHA, age, prior myocardial infarction (MI), and LVEF. Following accumulation of similar findings in several single-center small trials, Agostini et al performed a 290 patient, combined data reanalysis study from 6 European sites, showing that the only significant predictors of major cardiac events over 2 years were LVEF and H/M. As in Figure 4, particularly striking is the ability of H/M to risk stratify patients with LVEF $\leq$ 35% in a continuous fashion, with event rates ranging from <5% for those with HMR $\geq$ 2.18 to over 50% for those with HMR $\leq$ 1.45.[68]

Cardiac ^{123}I-*m*IBG WR has been investigated by Ogita et al, showing that patients with washout $\geq$27% had a 35% 4-year cardiac death rate compared with no deaths for a normal WR, and a threefold increase in HF hospital admissions in the high WR group.[55] Another study from this group reported that increased WR predicted SCD.[69]

Upon meta-analysis of literature from 18 prior studies, a total of 1,755 patients, Verberne et al reported that abnormal WR had a pooled hazard ratio (HR) of 1.72 ($P = .006$) for cardiac death, and a HR of 1.08 ($P < .001$) for cardiac events (cardiac death, MI, transplant, HF hospitalization); in the three best studies reported for late H/M, there was a HR of 1.82 ($P = .015$) for cardiac death and 1.98 ($P < .001$) for cardiac events.[70]

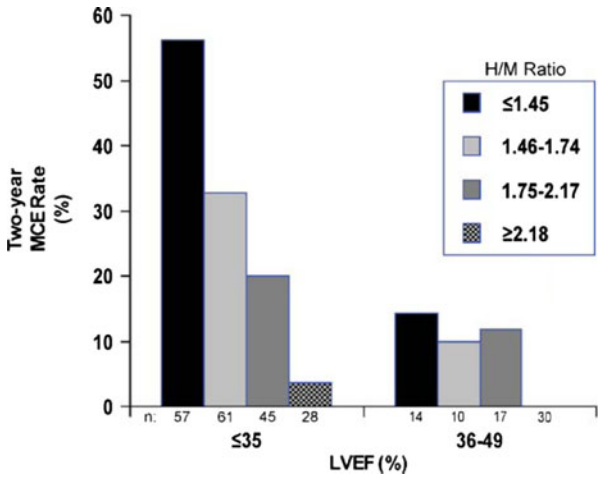

Figure 4. Major cardiac event rates (MCE) over 2 years in relation to left ventricular ejection fraction (LVEF) and ^{123}I-*m*IBG H/M. Cardiac events include cardiac death, transplant, and potentially lethal arrhythmias based on implantable cardioverter defibrillator discharge. Reprinted from Agostini et al[68] with kind permission from Springer Science and Business Media.

Efforts culminated in the AdreView Myocardial Imaging for Risk Evaluation in Heart Failure (ADMIRE-HF) trial, a prospective, multicenter, international study of 961 patients with NYHA Class II-III and LVEF $\leq$ 35%.[71] At 17-month follow-up, an H/M < 1.6 more than doubled—from 15% to 37%—the incidence of worsening NYHA class, life-threatening arrhythmias (sustained ventricular tachycardia >30 seconds, resuscitated cardiac arrest, and appropriate implantable cardioverter defibrillator (ICD) discharge), and cardiac death (CD), with a composite hazard ratio of 0.40 ($P < .001$) for a higher H/M. Multivariate analysis showed that H/M was a predictor of cardiac and all-cause deaths independent of other clinical and image variables, including age, NYHA functional class, LVEF, and brain natriuretic peptide (BNP). In particular, there were only 2 CDs for 201 patients (about 20% of total) who had H/M $\geq$ 1.6, including for ejection fraction (EF) <20%, thus a low negative predictive value of <1%, shown in Figure 5.[72] Although only one study, findings from ADMIRE-HF indicate that ^{123}I-*m*IBG imaging in otherwise high-risk HF patients can identify a significantly large subgroup who are in fact at low risk, at least over an approximately 2-year follow-up.

In a subanalysis of ADMIRE-HF patients, Ketchum et al[73] found that H/M added significantly to the prognostic power of the Seattle Heart Failure Model (SHFM),[74] an algorithm of routinely collected demographic, imaging, laboratory, and therapeutic parameters that determine the likely 1-5 year mortality. Adding H/M to the SHFM-D algorithm (modified by data from the SCD-HEFT -Sudden Cardiac Death in Heart Failure Trial)[75] yielded a net reclassification improvement of 22.7%, with 14.9% of subjects who died reclassified as higher risk, and 7.9% of patients who survived reclassified as lower risk, shown in Figure 6.[73]

Assessing Response to Therapy

Given concerns about overuse of medical testing, it is important that the risk stratification ability of a modality such as ^{123}I-*m*IBG imaging lead to improved patient outcome. Recent American College of Cardiology Foundation/American Heart Association HF guidelines recommend comprehensive pharmacologic regimens.[76] As mortality for CHF patients remains high,[77] when pharmacologic therapy is insufficient advanced mechanical device therapies such as biventricular pacemakers for cardiac resynchronization therapy (CRT), left ventricular assist devices (LVAD), and implantable cardiac defibrillators (ICD) should be considered, as well as cardiac

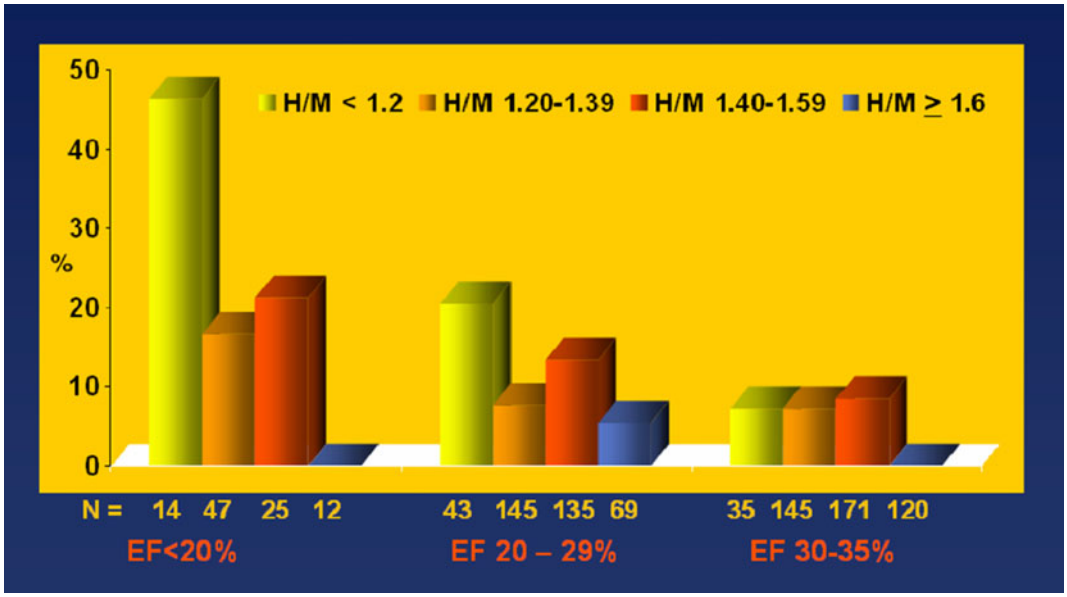

Figure 5. Relationship of left ventricular ejection fraction (EF) and H/M to 2-year cardiac mortality in the ADMIRE-HF study. Reprinted from Chirumamilla[15] with permission from Elsevier.

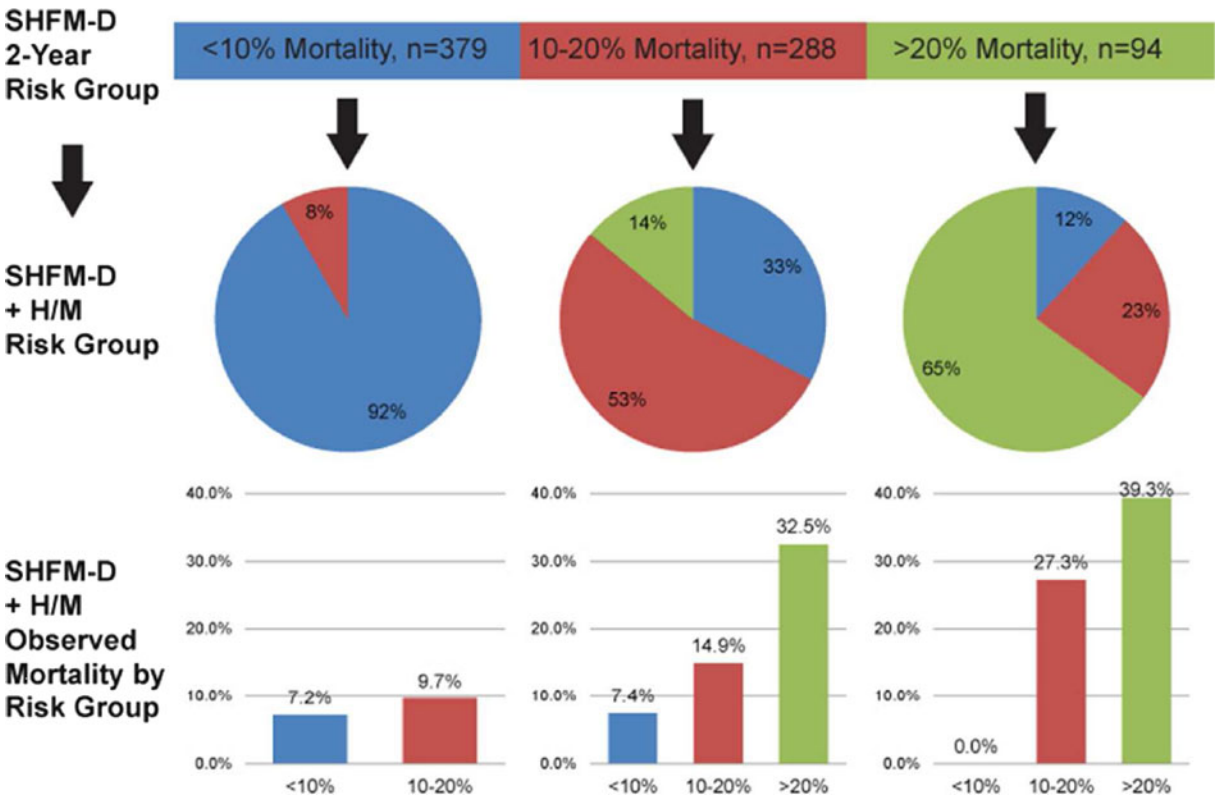

Figure 6. 2-Year-mortality risk reclassification enhancement when ^{123}I-*m*IBG H/M is added to the Seattle Heart Failure model (SHFM-D). The net re-classification improvement from image findings was 22.7%. Reprinted from Ketchum et al[73].

transplantation. To help better decide the need for advanced therapies, ways of assessing pharmacologic efficacy that might include a surrogate endpoint, such as improvement in an imaging study, should be useful. Much work has shown potential for ^{123}I-*m*IBG imaging to be effective in this regard. For example, numerous studies have shown that cardiac ^{123}I-*m*IBG images improve after therapy with β-blockers.[48,50,78-83] Gerson et al[50] showed that the H/M improved significantly after the use of carvedilol, especially in patients with an H/M ratio <1.40. Toyama et al[84] showed favorable changes of symptoms, functional class, cardiac function, and H/M in those treated with metoprolol. Kasama et al[85] reported on the therapeutic effect of carvedilol on ^{123}I-*m*IBG parameters and LV remodeling in patients with dilated cardiomyopathy.

Although improvement in autonomic function parameters in response to β-blockers is understandable, other medications, such as angiotensin-converting enzyme inhibitors (ACE-I), angiotensin receptor blockers (ARBs), and spironolactone that affect the renin-angiotensin system, also improve cardiac ^{123}I-*m*IBG uptake.[86-91] Amiodarone, an antiarrhythmic medication that would not be expected to directly influence cardiac sympathetic function, has also been shown to improve ^{123}I-*m*IBG parameters in patients with advanced HF.[92]

Many ask if ^{123}I-*m*IBG imaging might help direct medical therapy. Such investigations in terms of β-blockers have shown that imaging does not provide sufficient separation between those who do or do not benefit,[83,93] and given the high benefit/risk and relatively low cost of medical therapies, an ^{123}I-*m*IBG study is unlikely to preclude their use.[94] ^{123}I-*m*IBG imaging could instead be used to determine whether or not a particular therapy is working, perhaps increase doses more aggressively or determine if device therapies or transplantation are needed.[95,96] Matsui et al[97] studied patients with severe cardiomyopathy, and found that after 6 months of optimal medical therapy, a worsening H/M had, with BNP, the highest predictive value for CD, suggesting that such patients may have benefited from earlier device therapy or transplant. At the same time, a recent study by Drakos et al[98] of patients with an LVAD found that clinical improvement paralleled improvement in tracer uptake, suggesting that ^{123}I-*m*IBG could guide which patients need transplant, or instead who might be able to have the device discontinued. Along the same lines, it is reported that a decreased H/M predicted poor response to CRT.[99]

Cardiac Arrhythmias

A major cause of mortality in HF patients is SCD, most often from a ventricular arrhythmia.[100] SCD is particularly tragic in HF patients who otherwise have a reasonable quality of life. The currently accepted approach to potential SCD is an ICD, sometimes as secondary prevention after an aborted event, but increasingly more as primary prevention without specific evidence of risk. Recommended ICD use for primary prevention derives mostly from four large randomized studies: Multicenter Automatic Defibrillator Implantation Trial-II (MADIT-2),[101] Defibrillator in Acute Myocardial Infarction Trial (DINAMIT),[102] Defibrillators in Nonischemic Cardiomyopathy Treatment Evaluation (DEFINITE),[103] and SCD-HeFT.[74] HF guidelines assign a Class IA recommendation for implantation of an ICD as primary prevention in patients with NYHA Class II-III symptoms and LVEF $\leq$ 35%.[76]

LVEF has become a major variable for deciding who should receive an ICD, but this approach is flawed. One issue is that while the aforementioned trials indicate good relative survivals and significant *P*-values for ICD benefit, the absolute decreases in mortality are fairly small, from about 5.6% to 7.2%, with 11 to 14 patients needing an ICD to save 1 life.[74,101,104] This degree of benefit must be balanced against substantial risks and costs of an ICD.[105-108] The randomized trials have limitations, in particular MADIT-II and SCD-HEFT having broad enrollment criteria with limited stratification of study populations.[109] Differences among EF entry criteria were large, and most enrolled patients had EFs well below the threshold ultimately used in guidelines. Buxton et al[110] found that multiple factors other than LVEF provide more accurate prediction of SCD and mortality. Over half of the patients who die suddenly have an LVEF > 30%,[111-113] and thus guidelines do not recommend an ICD for the majority of patients who have SCD. In part, because of perceived guideline limitations, many clinicians are not following them.[114,115] Lack of clarity about a patient's true LVEF, often based on visual estimates ''subject to bias and reader error,'' often differing depending on the imaging method chosen, create more uncertainty.[109,116] Many feel that a better method of deciding on an ICD as primary prevention is needed.[117]

Autonomic imaging depicts cardiac pathophysiology closer to the underlying mechanisms of arrhythmias,[100,118] and there is much evidence that ^{123}I-*m*IBG imaging can effectively indicate which patients are likely to benefit from an ICD.[119] Arora et al.,[120] in a small study of 17 patients with advanced HF and an ICD, found that an H/M < 1.54 was associated with increased incidence of ICD discharges, and that on tomographic imaging patients who had ICD discharges had more extensive ^{123}I-*m*IBG defects and more extensive autonomic/perfusion mismatches, shown in Figure 7. An example of a SPECT images in a patient

with severe/extensive ^{123}I-*m*IBG defect(s) and autonomic/perfusion mismatch is seen in Figure 8. Subsequently, Nagahara et al[121] prospectively followed 54 patients with an ICD, finding that H/M correlated significantly and independently with appropriate discharges and SCD. Nishisato et al reported that a combination of H/M and the summed perfusion defect score on ^{99m}Tc-tetrosfomin images separated patients with ICD shocks from those without, with image variables independent and superior to age, sex, SAECG, BNP, medications, inducible arrhythmias, and LVEF in predicting shocks or cardiac death.[122] Kasama et al[123] showed a correlation of abnormally high ^{123}I-*m*IBG washout with increased SCD. Tamaki et al. compared ECG parameters—HRV, QT dispersion, and SAECG—with ^{123}I-*m*IBG findings in 106 patients with LVEF $< 40\%$, and those with SCD had a lower H/M and higher WR, with ECG variables showing no independent relationship to outcome.[124] In ADMIRE-HF, combined arrhythmic events were more common in subjects with H/M < 1.60 (10.4%) than in those with H/M ≥ 1.6 (3.5%, $P < 0.01$).[71] In a subanalysis of 578 patients without an ICD, Senior et al[125] reported only one fatal arrhythmic event in patients with H/M ≥ 1.60. In terms of tomographic imaging, Bax et al[59] reported that in patients with prior MI, the extent/severity (summed score) of ^{123}I-*m*IBG defects correlated with electrophysiological VT inducibility, and Boogers et al. found that in HF patients with a mean LVEF of 28% who received an ICD, a summed score >26 independently predicted more frequent ICD discharges and cardiac death (13-fold higher risk).[126] Interestingly neither of these latter two studies found a correlation of autonomic/perfusion mismatch with pre-disposition to arrhythmias.

Thus, there are consistent findings that ^{123}I-*m*IBG images can predict ICD discharges and SCD independent of conventional variables. In particular, a satisfactory H/M has an extremely high negative predictive value. Nevertheless, it is understood that larger prospective studies are needed before there can be wide acceptance and inclusion of ^{123}I-*m*IBG imaging in guidelines.[127] At the same time, cardiac neuronal imaging could potentially identify a subgroup of patients thought of as lower risk (e.g., LVEF $> 35\%$), but who are instead at significant risk of SCD and may need an ICD.

^{123}I-*m*IBG imaging might also help evaluate patients with primary arrhythmias. Mitrani et al[128] observed that in patients who presented with VT but had structurally normal hearts, 55% had regional sympathetic denervation compared with none of the control patients. Gill et al[129] found asymmetrical uptake of ^{123}I-*m*IBG (less in septum) in 47% of patients with VT and ''clinically normal'' hearts, particularly obvious in patients with exercise-induced VT.

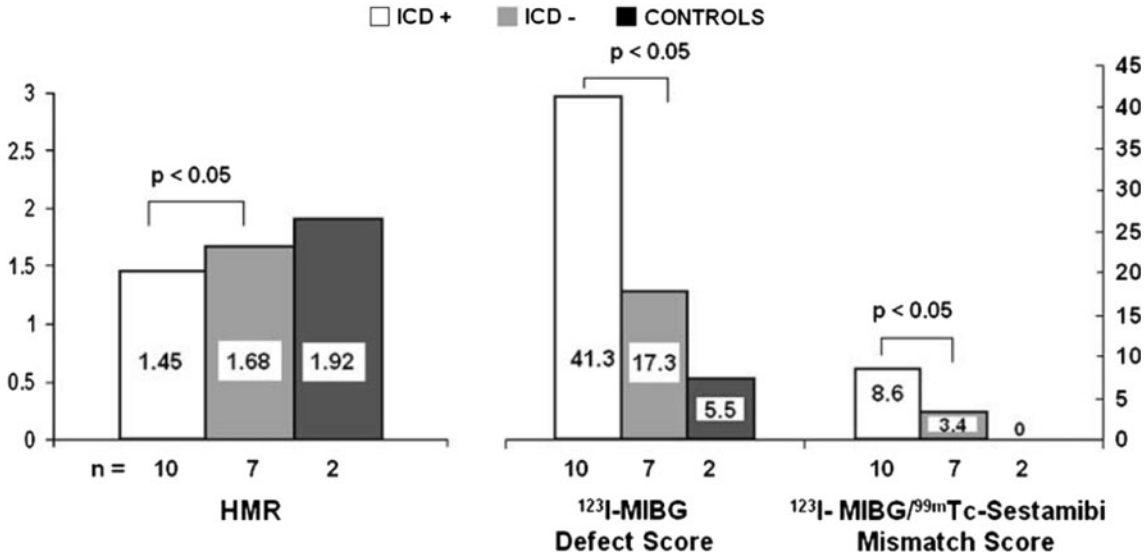

Figure 7. Planar and SPECT ^{123}I-mIBG results in relation to the occurrence of implantable cardioverter defibrillator (ICD) discharges in 17 patients with ICDs and 2 control patients without heart disease. Compared with patients who did not have an ICD discharge (ICD− patients with a discharge (ICD+) had a lower mean HMR, a higher mean neuronal tracer defect score, and a higher mean neuronal tracer uptake/perfusion tracer mismatch score. Reprinted from Cardiology Clinics: Nuclear Cardiology—From Perfusion to Tissue Biology, Vol. 27, Travin[19] with permission from Elsevier.

Interestingly, PET autonomic tracer (i.e., ^{11}C-HED) imaging of particular primary arrhythmias, such as right ventricular outflow tract tachycardia[130] and Brugada syndrome, shows focal defects in specific myocardial walls.[131] Regional autonomic abnormalities can also be seen in nonischemic cardiomyopathies, such as Chagas disease in which the posterolateral, inferior, and apical walls are selectively affected. In one study of 26 patients with chronic Chagas cardiomyopathy, ^{123}I-*m*IBG defects correlated with the occurrence of sustained VT.[132] Further investigation of such observations may lead to better understanding of the pathophysiology of cardiac autonomic innervation, as well as the particular disease entities.

Ischemic Heart Disease

^{123}I-*m*IBG imaging also shows promise in the setting of ischemic heart disease. Sympathetic fibers are more sensitive to ischemia than myocytes.[133] MI causes sympathetic denervation beyond the infarcted area.[56,134-137] Injury to sympathetic innervation may persist after myocyte recovery, resulting in areas of autonomic/perfusion mismatch, possibly pre-disposing to post-MI arrhythmias.[57,138-140] Tomoda et al[141] showed that 3-4 weeks after nonST segment elevation MI, ^{123}I-*m*IBG defects may be present without Tl-201 perfusion defects. ^{123}I-*m*IBG defects can occur following angina,[142] and may be present up to 6 months after coronary spasm.[143,144] Simula et al[145] reported potential use in detecting subclinical disease, finding autonomic image abnormalities in asymptomatic patients with normal ^{99m}Tc-sestamibi studies but with left anterior descending disease. Subclinical endothelial dysfunction may cause episodes of vasoconstriction, resulting in neurohormonal event sequences that affect local sympathetic output.

^{123}I-*m*IBG imaging can also shed light on the effect of sympathetic alteration on post-MI LV remodeling. Sakata et al[146] found that after a first MI, despite a patent infarct coronary artery, the presence of a high severity score correlated with LV end-systolic volume dilatation.

Autonomic imaging is under investigation in the setting of ''hibernating'' myocardium. Using a porcine model, Luisi et al[147-150] have produced large regional autonomic defects that increase in size and severity over time, increasing the likelihood of arrhythmic SCD. Similar abnormalities in sympathetic nerve function in chronic ischemic disease without infarction have been described in humans, such as Hartikainen et al[151] finding

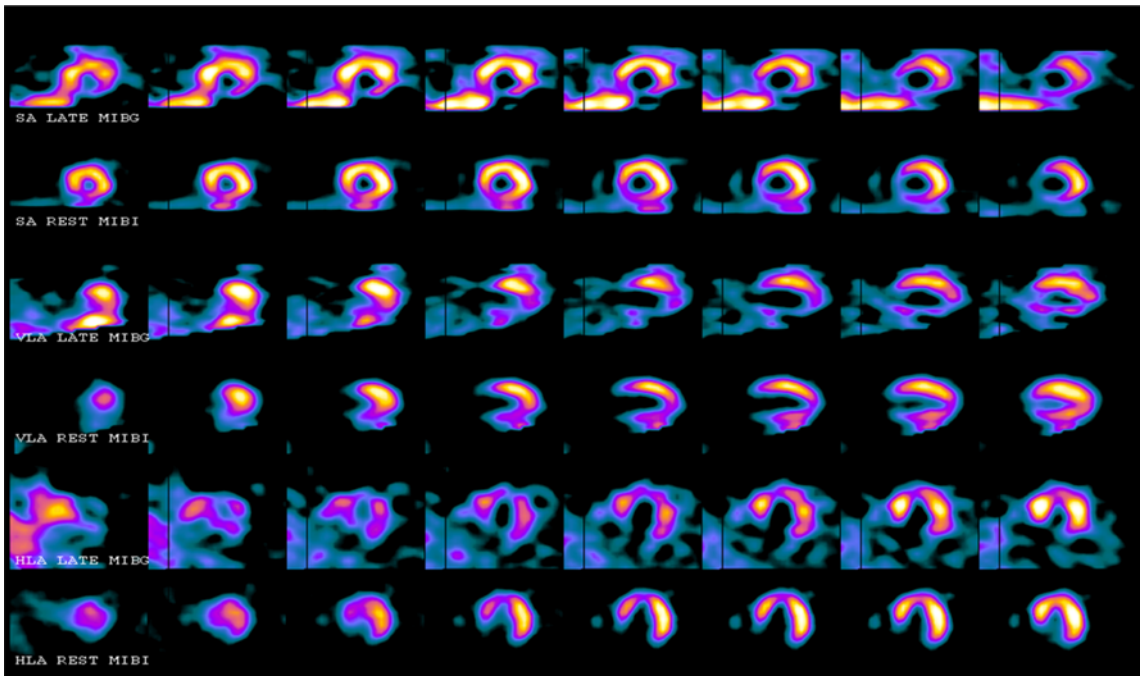

Figure 8. ^{123}I-*m*IBG and ^{99m}Tc-sestamibi SPECT images of a patient who had received numerous appropriate ICD shocks. There are neuronal/perfusion mismatching defects involving the inferior, inferolateral, and apical walls; there is a matched defect in the anterior wall. *HLA*, Horizontal long axis; *ICD*, implantable cardioverter defibrillator; *MIBG*, metaiodobenzylguanidine (^{123}I-*m*IBG); *MIBI*, ^{99m}Tc-sestamibi; *SA*, short axis. Reprinted from Ji and Travin[20] with kind permission from Springer Science and Business Media.

regional ^{123}I-*m*IBG defects in almost all patients with a >50% coronary stenosis. Among those with a stenosis >90%, ^{123}I-*m*IBG defect size was indistinguishable from patients with previous MI.

To examine further the utility of autonomic imaging in hibernating myocardium, the Prediction of ARrhythmic Events with Positron Emission Tomography (PAREPET) trial has been undertaken. In this observational cohort study, >200 patients with ischemic cardiomyopathy (NYHA Class I-III CHF, EF $\leq$ 35%), without plans for coronary revascularization, underwent $^{13}NH_3$ PET perfusion imaging, ^{18}FDG myocardial viability imaging, and ^{11}C-HED imaging.[152] Preliminary data demonstrate significant variability in the extent of viable, dysinnervated myocardium, from small borders around areas of infarction to large confluent regions encompassing several myocardial segments.[153] At the 2012 Heart Rhythm Society meetings, Fallavollita reported that the 4-year occurrence of sudden cardiac arrest (arrhythmic death or ICD shock for VT $\geq$ 240 minutes or ventricular fibrillation) increased in relation to the severity/extent of autonomic image abnormalities independent of BNP, CHF symptoms, or LVEF; of note autonomic/perfusion mismatch was not an independent predictor of adverse outcome.[154] While this work was with a PET autonomic tracer, similar principles should apply to imaging with ^{123}I-*m*IBG.

Autonomic Imaging in Other Conditions

Autonomic imaging has been shown to have potential use in other clinical conditions. Akutsu et al[155] found that in HF patients with paroxysmal atrial fibrillation (AF), a decreased H/M was independently predictive of transition to permanent AF.

Following cardiac transplant reinnervation is important, and its absence may indicate cardiac pathology.[156] Estorch et al[157] studied patients 6 months to 12 years post-transplant, finding that H/M correlated with time after transplantation, indicating progressive reinnervation. Patients with absent tracer uptake were more likely to develop coronary vasculopathy.

Numerous reports have shown that in diabetic patients, uptake abnormalities of ^{123}I-*m*IBG or PET autonomic tracers correlate with a worsened prognosis, even in the absence of clinical neuropathy.[158,159] Nagamachi et al[160] followed 144 patients without evidence of heart disease for 7.2 years, finding that a combination of decreased H/M and heart rate variability (HRV) abnormalities independently predicted events, and delayed H/M alone predicted all-cause mortality. Yufu et al[161] reported that abnormal ^{123}I-*m*IBG washout and age were independently associated with major cardiac and cerebrovascular events. Further work should determine if neuronal imaging in diabetics can effectively detect higher risk than is clinically apparent.

Given the enhanced sensitivity of sympathetic nerve to insults, some have investigated potential use of autonomic imaging to identify early myocardial damage from cancer chemotherapy. Olmos et al[162] found decreased ^{123}I-*m*IBG uptake as the cumulative dose of doxorubicin increased, with subsequent deterioration in LVEF. Carrió and colleagues found that at a cumulative doxorubicin dose of 240-300 mg/m^2 ^{123}I-*m*IBG abnormalities correlated with ^{111}In-antimyosin antibody uptake, although they found no association with LV functional impairment.[163] Clinical utility beyond current monitoring methods needs further investigation.

LOOKING FORWARD

Prospective studies in larger study populations are required to establish the clinical utility of ^{123}I-*m*IBG imaging in the various clinical scenarios discussed such that it is accepted by general cardiologists and allied physicians. It is important to demonstrate that the technique can effectively guide therapy to improve patient outcome and well being. Given that cardiac autonomic innervation is linked to underlying molecular and electrophysiologic processes of disease, radionuclide autonomic imaging promises to yield information that other imaging techniques cannot. Autonomic imaging may provide unexpected insights and understanding of cardiac diseases, and lead to new therapies. It is important that those in the field of nuclear cardiology encourage and participate in the development of this method.

References

1. Klocke FJ, Baird MG, Lorell BH, Bateman TM, Messer JV, Berman DS, et al. ACC/AHA/ASNC guidelines for the clinical use of cardiac radionuclide imaging—executive summary: A report of the American College of Cardiology/American Heart Association Task Force on Practice Guidelines (ACC/AHA/ASNC Committee to Revise the 1995 Guidelines for the Clinical Use of Radionuclide Imaging). J Am Coll Cardiol 2003;42:1318-33.
2. Shaw LJ, Iskandrian AE. Prognostic value of gated myocardial perfusion SPECT. J Nucl Cardiol 2004;11:171-85.
3. Hamad EA, Travin MI. The complementary roles of radionuclide myocardial perfusion imaging and cardiac computed tomography. Semin Roentgenol 2012;47:228-39.
4. Iskander S, Iskandrian AE. Risk assessment using single-photon emission computed tomographic technetium-99m sestamibi imaging. J Am Coll Cardiol 1998;32:57-62.
5. Hachamovitch R, Berman DS, Shaw LJ. Incremental prognostic value of myocardial perfusion single photon emission computed tomography for the prediction of cardiac death: Differential

stratification for risk of cardiac death and myocardial infarction. Circulation 1998;97:535-43.
6. Hachamovitch R, Hayes SW, Friedman JD, Cohen I, Berman DS. Comparison of the short-term survival benefit associated with revascularization compared with medical therapy in patients with no prior coronary artery disease undergoing stress myocardial perfusion single photon emission computed tomography. Circulation 2003;107:2900-6.
7. Hachamovitch R, Berman DS. The use of nuclear cardiology in clinical decision making. Semin Nucl Med 2005;35:62-72.
8. Sharir T, Germano G, Kang X, Lewin HC, Miranda R, Cohen I, et al. Prediction of myocardial infarction versus cardiac death by gated myocardial perfusion SPECT: Risk stratification by the amount of stress-induced ischemia and the poststress ejection fraction. J Nucl Med 2001;42:831-7.
9. Travin MI, Bergmann SR. Assessment of myocardial viability. Semin Nucl Med 2005;35:2-16.
10. Mielniczuk LM, Beanlands RS. Imaging-guided selection of patients with ischemic heart failure for high-risk revascularization improves identification of those with the highest clinical benefit. Circ Cardiovasc Imaging 2012;5:262-70.
11. Shaw LJ, Berman DS, Maron DJ, et al. Optimal medical therapy with or without percutaneous coronary intervention to reduce ischemic burden. Results from the clinical outcomes utilizing revascularization and aggressive drug evaluation (COURAGE) trial nuclear substudy. Circulation 2008;117:1283-91.
12. Bengel FM. Clinical cardiovascular molecular imaging. J Nucl Med 2009;50:837-40.
13. Morrison AR, Sinusas AJ. Advances in radionuclide molecular imaging in myocardial biology. J Nucl Cardiol 2010;17:116-34.
14. Sinusas AJ, Thomas JD, Mills G. The future of molecular imaging. J Am Coll Cardiol Imag 2011;4:799-806.
15. Chirumamilla A, Travin MI. Cardiac applications of 123I-mIBG imaging. Semin Nucl Med 2011;41:374-87.
16. Kapa S, Somers VK. Cardiovascular manifestations of autonomic disorders. In: Libby P, Bonow RO, Mann DL, Zipes DP, Braunwald E, editors. Braunwald's heart disease: A textbook of cardiovascular medicine. 8th ed. Philadelphia: Saunders Elsevier; 2008. p 2171-83.
17. Zipes DP. Autonomic modulation of cardiac arrhythmias. In: Zipes DP, Jalife J, editors. Cardiac electrophysiology: from cell to bedside. 2nd ed. Philadelphia: W.B. Saunders Company; 1995. p. 441-2.
18. Carrió I. Cardiac neurotransmission imaging. J Nucl Med 2001;42:1062-76.
19. Travin MI. Cardiac neuronal imaging at the edge of clinical application. Cardiol Clin 2009;27:311-27.
20. Ji SY, Travin MI. Radionuclide imaging of cardiac autonomic innervation. J Nucl Cardiol 2010;17:655-66.
21. Verrier RL, Antzelevich C. Autonomic aspects of arrhythmogenesis: The enduring and the new. Curr Opin Cardiol 2004;19:2-11.
22. Flotats A, Carrió I. Cardiac neurotransmission SPECT imaging. J Nucl Cardiol 2004;11:587-602.
23. Sisson JC, Wieland DM. Radiolabeled meta-iodobenzylguanidine pharmacology: Pharmacology and clinical studies. Am J Physiol Imaging 1986;1:96-103.
24. Bengel FM, Schwaiger M. Assessment of cardiac sympathetic neuronal function using PET imaging. J Nucl Cardiol 2004;11:603-16.
25. Raffel DM, Wieland DM. Development of mIBG as a cardiac innervation imaging agent. J Am Coll Cardiol Imaging 2010;3:111-6.
26. Counsell RE, Yu T, Ranade VV, Buswink Am, Carr EA, Carroll M. Radioiodinated bretylium analogs for myocardial scanning. J Nucl Med 1974;15:991-6.
27. Korn N, Buswink A, Yu T, Carr EA, Carroll M, Counsell RE. A radioiodinated bretylium analog as a potential agent for scanning the adrenal medulla. J Nucl Med 1977;18:87-9.
28. Wieland DM, Mangner TJ, Inbasekaran MN, Brown LA, Wu J. Adrenal medulla imaging agents: A structure distribution relationship study of radiolabeled aralkkylguandines. J Med Chem 1984;27:149-55.
29. Kline RC, Swanson DP, Wieland DM, Thrall JH, Gross MD, Pitt B, et al. Myocardial imaging in man with I-123 meta-iodobenzylguanidine. J Nucl Med 1981;22:129-32.
30. Sisson J, Shapiro B, Meyers L, Mallette S, Mangner TJ, Wieland DM, et al. Metaiodobenzylguanidine to map scintigraphically the adrenergic nervous system in man. J Nucl Med 1987;28:1625-36.
31. Sisson JC, Lynch JJ, Johnson J, Jaques S Jr, Wu D, Bolgos G, et al. Scintigraphic detection of regional disruption of adrenergic neurons in the heart. Am Heart J 1988;116:67-76.
32. Rabinovitch MA, Rose CP, Schwab AJ, Fitchett DH, Honos GN, Stewart JA, et al. A method of dynamic analysis of iodine-123-meta-iodobenzylguanidine scintigrams in cardiac mechanical overload hypertrophy and failure. J Nucl Med 1993;34:589-600.
33. Nakajo M, Shapiro B, Glowniak J, Sisson JC, Beierwaltes WH. Inverse relationship between cardiac accumulation of meta-[^{131}I] iodobenzylguanidine (I-131 MIBG) and circulating catecholamines in suspected pheochromocytoma. J Nucl Med 1983;24:1127-34.
34. Nakajo M, Shimabukuro K, Yoshimura H, Yonekura R, Nakabeppu Y, Tanoue P, et al. Iodine-131 metaiodobenzylguanidine intra- and extravesicular accumulation in the rat heart. J Nucl Med 1986;27:84-9.
35. Hattori N, Schwaiger M. Metaiodobenzylguanidine scintigraphy of the heart. What have we learned clinically? Eur J Nucl Med 2000;27:1-6.
36. Flotats A, Carrió I, Agostini D, Le Guludec D, Marcassa C, Schaffers M, et al. Proposal for standardization of ^{123}I-metaiodobenzylguanidine (MIBG) cardiac sympathetic imaging by the EANM Cardiovascular Committee and the European Council of Nuclear Cardiology. Eur J Nucl Med Mol Imaging 2010;37:1802-12.
37. Jacobson AF, Lombard J, Banerjee G, Camici PG. ^{123}I-*m*IBG scintigraphy to predict risk for adverse cardiac outcomes in heart failure patients: Design of two prospective multicenter international trials. J Nucl Cardiol 2009;16:113-21.
38. Yamashina S, Yamazaki J. Neuronal imaging using SPECT. Eur J Nucl Med Mol Imaging 2007;34:S62-73.
39. Agostini D, Carrió I, Verberne HJ. How to use 123I-MIBG scintigraphy in chronic heart failure. Eur J Nucl Med Mol Imaging 2009;36:555-9.
40. Carrió I, Cowie MR, Yamazaki J, Udelson J, Camici PG. Cardiac sympathetic imaging with mIBG in heart failure. J Am Coll Cardiol Imaging 2010;3:91-100.
41. Solanki KK, Bomanji J, Moyes J, Mather SJ, Trainer PJ, Britton KE. A pharmacological guide to medicine which interfere with the biodistribution of radiolabelled meta-iodobenzylguanidine (MIBG). Nucl Med Commun 1992;13:513-21.
42. Wafelman AR, Hoefnagel CA, Maes RA, Beijnen JH. Radioiodinated metaiodobenzylguanidine: A review of its biodistribution and pharmacokinetics, drug interaction, cytotoxicity and dosimetry. Eur J Nucl Med 1994;21:545-59.
43. Inoue Y, Suzuki A, Shirouzu I, Machida T, Yoshizawa Y, Akita F, et al. Effect of collimator choice on quantitative assessment of

cardiac iodine 123 MIBG uptake. J Nucl Cardiol 2003;10:623-32.
44. Verberne HJ, Feenstra C, de Jong WM, Somsen GA, Van Eck-Smit BL, Busemann Sokole E. Influence of collimator choice and simulated clinical conditions on 123I-MIBG heart/mediastinum ratios: A phantom study. Eur J Nucl Med Mol Imaging 2005;32:1100-7.
45. Chen J, Garcia EV, Galt JR, Folks RD, Carrio I. Optimized acquisition and processing protocols for I-123 cardiac SPECT imaging. J Nucl Cardiol 2006;13:251-60.
46. Chen J, Garcia EV, Galt JR, Folks RD, Carrió I. Improved quantification in I-123 cardiac SPECT imaging with deconvolution of septal penetration. Nucl Med Commun 2006;27:551-8.
47. Chen JI, Folks RD, Verdes L, Manatunga DN, Jacobson AF, Garcia EV. Quantitative I-123 mIBG SPECT in differentiating abnormal and normal mIBG myocardial uptake. J Nucl Cardiol 2012;19:92-9.
48. Agostini D, Belin A, Amar MH, Darlas Y, Hamon M, Grollier G, et al. Improvement of cardiac neuronal function after carvedilol treatment in dilated cardiomyopathy: A ^{123}I-MIBG scintigraphic study. J Nucl Med 2000;41:845-51.
49. Yamada T, Shimonagata T, Fukunami M, Kumagai K, Ogita H, Hirata A, et al. Comparison of the prognostic value of cardiac iodine-123 metaiodobenzylguanidine imaging and heart rate variability in patients with chronic heart failure. J Am Coll Cardiol 2003;41:231-8.
50. Gerson MC, Craft LL, McGuire N, Suresh DP, Abraham WT, Wagoner LE. Carvedilol improves left ventricular function in heart failure with idiopathic dilated cardiomyopathy and a wide range of sympathetic nervous system function as measured by iodine 123 metaiodobenzylguanidine. J Nucl Cardiol 2002;9:608-15.
51. Okuda K, Nakajima K, Hosoya T, Ishikawa T, Konishi T, Matsubara K, et al. Semi-automated algorithm for calculating heart-to-mediastinum ratio in cardiac Iodine-123 MIBG imaging. J Nucl Cardiol 2011;18:82-9.
52. Chen GP, Tabibiazar R, Branch KR, Link JM, Caldwell JH. Cardiac receptor physiology and imaging: An update. J Nucl Cardiol 2005;12:714-30.
53. Morozumi T, Kusuoka H, Fukuchi K, Tani A, Uehara T, Matsuda S, Tsujimura E, et al. Myocardial iodine-123-metaiodobenzylguanidine images and autonomic nerve activity in normal subjects. J Nucl Med 1997;38:49-52.
54. Somsen GA, Verberne HJ, Fleury E, Righetti A. Normal values and within-subject variability of cardiac I-123 MIBG scintigraphy in healthy individuals: Implications for clinical studies. J Nucl Cardiol 2004;11:126-33.
55. Ogita H, Shimonagata T, Fukunami M, Kumagai K, Yamada T, Asano Y, et al. Prognostic significance of cardiac ^{123}I metaiodobenzylguanidine imaging for mortality and morbidity in patients with chronic heart failure: A prospective study. Heart 2001;86:656-60.
56. Minardo JD, Tuli MM, Mock BH, Weiner RE, Pride HP, Wellmann HN, et al. Scintigraphic and electrophysiologic evidence of canine myocardial sympathetic denervation and reinnervation produced by myocardial infarction or phenol application. Circulation 1988;78:1008-19.
57. Simões MV, Barthel P, Matsunari I, Nekolla SG, Schömig A, Schwaiger M, et al. Presence of sympathetically denervated but viable myocardium and its electrophysiologic correlates after early revascularised, acute myocardial infarction. Eur Heart J 2004;25:551-7.
58. Cerqueira MD, Weissman NJ, Dilsizian V, Jacobs AK, Kaul S, Laskey WK, et al. Standardized myocardial segmentation and nomenclature for tomographic imaging of the heart. A statement for healthcare professionals from the Cardiac Imaging Committee of the Council on Clinical Cardiology of the American Heart Association. Circulation 2002;105:539-42.
59. Bax JJ, Kraft O, Buxton AE, Fjeld JG, Parizek P, Agostini D, et al. ^{123}I-*m*IBG Scintigraphy to predict inducibility of ventricular arrhythmias on cardiac electrophysiology testing: A prospective multicenter pilot study. Circ Cardiovasc Imaging 2008;1:131-40.
60. Tsuchimochi S, Tamaki N, Tadamura E, Kawamoto M, Fujita T, Yonekura Y, et al. Age and gender differences in normal myocardial adrenergic neuronal function evaluated by iodine-123-MIBG imaging. J Nucl Med 1995;36:969-74.
61. Estorch M, Serra-Grima R, Flotats A, Marí C, Bernà L, Catafau A, et al. Myocardial sympathetic innervation in the athlete's sinus bradycardia. Is there selective inferior myocardial wall denervation? J Nucl Cardiol 2000;7:354-8.
62. Bulow HP, Stahl F, Lauer B, Nekolla SG, Schuler G, Schwaiger M, et al. Alterations of myocardial presynaptic sympathetic innervation in patients with multi-vessel coronary artery disease but without history of myocardial infarction. Nucl Med Commun 2003;24:233-9.
63. Roger VI, Go AS, Lloyd-Jones DM, Benjamin EJ, Barry JD, Borden WB, et al. Heart disease and stroke statistics—2012 update: A report from the American Heart Association. Circulation 2012;2012:e2-220.
64. Triposkiadis F, Karayannis G, Giamouzis G, Skoularigis J, Louridas G, Butler J. The sympathetic nervous system in heart failure physiology, pathophysiology, and clinical implications. J Am Coll Cardiol 2009;54:1747-62.
65. Schofer J, Spielmann R, Schuchert A, Weber K, Schlüter M. Iodine-123 meta-iodobenzylguanidine scintigraphy: A noninvasive method to demonstrate myocardial adrenergic nervous system disintegrity in patients with idiopathic dilated cardiomyopathy. J Am Coll Cardiol 1988;12:1252-8.
66. Merlet P, Valette H, Dubois-Randé J, Moyse D, Duboc D, Dove P, et al. Prognostic value of cardiac metaiodobenzylguanidine in patients with heart failure. J Nucl Med 1992;33:471-7.
67. Nakata T, Miyamoto K, Doi A, Sasao H, Wakabayashi T, Kobayashi H, et al. Cardiac death prediction and impaired cardiac sympathetic innervation assessed by MIBG in patients with failing and nonfailing hearts. J Nucl Cardiol 1998;5:579-90.
68. Agostini D, Verberne HJ, Burchert W, Knuuti J, Povinec P, Sambuceti G, et al. I-123-*m*IBG myocardial imaging for assessment of risk for a major cardiac event in heart failure patients: Insights from a retrospective European multicenter study. Eur J Nucl Med Mol Imaging 2008;35:535-46.
69. Kioka H, Yamada T, Mine T, Morita T, Tsukamoto Y, Tamaki S, et al. Prediction of sudden death in patients with mild-to-moderate chronic heart failure by using cardiac iodine-123 metaiodobenzylguanidine imaging. Heart 2007;93:1213-8.
70. Verberne HJ, Brewster LM, Somsen GA, van Eck-Smit BL. Prognostic value of myocardial 123I-metaiodobenzylguanidine (MIBG) parameters in patients with heart failure: A systematic review. Eur Heart J 2008;29:1147-59.
71. Jacobson AF, Senior R, Cerqueira MD, Wong ND, Thomas GS, Lopez VA, et al. Myocardial iodine-123 meta-iodobenzylguanidine imaging and cardiac events in heart failure. Results of the prospective ADMIRE-HF (AdreView Myocardial Imaging for Risk Evaluation in Heart Failure) study. J Am Coll Cardiol 2010;55:2212-21.
72. Travin M, Anathassubramaniam K, Henzlova MJ, Clements IP, Amanullah A, Jacobson AF. Imaging of myocardial sympathetic innervation for prediction of cardiac and all-cause mortality in

heart failure: Analysis from the ADMIRE-HF trial. Circulation 2009;120:S350.
73. Ketchum E, Jacobson A, Caldwell J, Senior R, Cerqueira M, Thomas G, et al. Selective improvement in Seattle heart failure model risk stratification using iodine-123 meta-iodobenzylguanidine imaging. J Nucl Cardiol 2012;19:1007-16.
74. Levy WC, Mozaffarian D, Linker DT, Sutradhar SC, Anker SD, Cropp AB, et al. The Seattle Heart Failure Model. Prediction of survival in heart failure. Circulation 2006;113:1424-33.
75. Bardy GH, Lee KL, Mark DB, Poole JE, Packer DL, Boineau R, et al. Amiodarone or an implantable cardioverter-defibrillator for congestive heart failure. N Engl J Med 2005;352:225-37.
76. Jessup M, Abraham WT, Casey DE, Feldman AM, Francis GS, Ganiats TG, et al. 2009 focused update: ACCF/AHA guidelines for the diagnosis and management of heart failure in adults: a report of the American College of Cardiology/American Heart Association Task Force on Practice Guidelines. J Am Coll Cardiol 2009;53:1343-82.
77. Roger VI, Weston SA, Redfield MM, Hellermann-Homan JP, Killian J, Yawn BP, et al. Trends in heart failure incidence and survival in a community-based population. JAMA 2004;292:344-50.
78. Merlet P, Pouillart F, Dubois-Randé J, Delahaye N, Fumey R, Castaigne A, et al. Sympathetic nerve alterations assessed with 123I-MIBG in the failing human heart. J Nucl Med 1999;40:224-31.
79. Cohen-Solal A, Rouzet F, Berdeaux A, Le Guludec D, Abergel E, Syrota A, et al. Effects of carvedilol on myocardial sympathetic innervations in patients with chronic heart failure. J Nucl Med 2005;46:1796-803.
80. Fujimoto S, Inoue A, Hisatake S, Yamashina S, Yamashina H, Nakano H, et al. Usefulness of 123I-metaiodobenzylguanidine myocardial scintigraphy for predicting the effectiveness of beta blockers in patients with dilated cardiomyopathy from the standpoint of long-term prognosis. Eur J Nucl Med Mol Imaging 2004;31:1356-61.
81. Fukuoka S, Hayashida K, Hirose Y. Use of MIBG myocardial imaging to predict the effectiveness of beta-blocker therapy in patients with dilated cardiomyopathy. Eur J Nucl Med 1997;24:523-9.
82. Lotze U, Kaepplinger S, Kober A, Richartz BM, Gottschild D, Figulla HR. Recovery of the cardiac adrenergic nervous system after longterm β-blocker therapy in idiopathic dilated cardiomyopathy: Assessment by increase in myocardial 123I-metaiodobenzylguanidine uptake. J Nucl Med 2001;42:49-54.
83. Suwa M, Otake Y, Moriguchi A, Ito T, Hirota Y, Kawamura K, et al. Iodine-123 metaiodobenzylguanidine myocardial scintigraphy for prediction of response to β-blocker therapy in patients with dilated cardiomyopathy (erratum in Am Heart J 1997; 134:1141). Am Heart J 1997;133:353-8.
84. Toyama T, Aihara Y, Iwasaki T, Hasegawa A, Suzuki T, Nagai R, et al. Cardiac sympathetic activity estimated by 123I-MIBG myocardial imaging in patients with dilated cardiomyopathy after β-blocker or angiotensin-converting enzyme inhibitor therapy. J Nucl Med 1999;40:217-23.
85. Kasama S, Toyama T, Hatori T, Sumino H, Kumakura H, Takayama Y, et al. Evaluation of cardiac sympathetic nerve activity and left ventricular remodeling in patients with dilated cardiomyopathy on the treatment containing carvedilol. Eur Heart J 2007;28:989-95.
86. Kasama S, Toyama T, Kumakura H, Takayama Y, Ichikawa S, Suzuki T, et al. Spironolactone improves cardiac sympathetic nerve activity and symptoms in patients with congestive heart failure. J Nucl Med 2002;43:1279-85.
87. Kasama S, Toyama T, Kumakura H, et al. Effect of spironolactone on cardiac sympathetic nerve activity and left ventricular remodeling in patients with dilated cardiomyopathy. J Am Coll Cardiol 2003;41:574-81.
88. Kasama S, Toyama T, Kumakura H. Effects of candesartan on cardiac sympathetic nerve activity in patients with congestive heart failure and preserved LVEF. J Am Coll Cardiol 2005;45:661-7.
89. Kasama S, Toyama T, Kumakura H, Takayama Y, Ichikawa S, Suzuki T, et al. Addition of valsartan to an angiotensin-converting enzyme inhibitor improves cardiac sympathetic nerve activity and left ventricular function in patients with congestive heart failure. J Nucl Med 2003;44:884-90.
90. Somsen GA, Vlies BV, de Milliano PA, Borm JJ, van Royen EA, Endert E, et al. Increased myocardial [123-I]-metaiodobenzylguanidine uptake after enalapril treatment in patients with chronic heart failure. Heart 1996;76:218-22.
91. Takeishi Y, Atsumi H, Fujiwara S, Takahashi K, Tomoike H. ACE inhibition reduces cardiac iodine-123-MIBG release in heart failure. J Nucl Med 1997;38:1085-9.
92. Toyama T, Hoshizaki H, Seki R, Isobe N, Adachi H, Naito S, et al. Efficacy of amiodarone treatment on cardiac symptom, function, and sympathetic nerve activity in patients with dilated cardiomyopathy: Comparison with β-blocker therapy. J Nucl Cardiol 2004;11:134-41.
93. Choi JY, Lee KH, Hong KP, Kim BT, Seo JD, Lee WR, et al. Iodine-123 MIBG imaging before treatment of heart failure with carvedilol to predict improvement of left ventricular function and exercise capacity. J Nucl Cardiol 2001;8:4-9.
94. Udelson JE, Shafer CD, Carrió I. Radionuclide imaging in heart failure: Assessing etiology and outcomes and implications for management. J Nucl Cardiol 2002;9:S40-52.
95. Merlet P, Benvenuti C, Moyse D, Pouillart F, Dubois-Randé J, Duval A, et al. Prognostic value of MIBG imaging in idiopathic dilated cardiomyopathy. J Nucl Med 1999;40:917-23.
96. Waqar F, Dunlap SH, Gerson MC. What will be the role of I-123 MIBG in improving the outcome of medically treated heart failure patients? J Nucl Cardiol 2012. doi:10.1007/s12350-012-9612z.
97. Matsui T, Tsutamoto T, Maeda K, Kusukawa J, Kinoshita M. Prognostic value of repeated ^{123}I-metaiodobenzylguanidine imaging in patients with dilated cardiomyopathy with congestive heart failure before and after optimized treatments—comparison with neurohumoral factors. Circ J 2002;66:537-43.
98. Drakos SG, Athanasoulis T, Malliaras KG, Terrovitis JV, Diakos N, Koudoumas D, et al. Myocardial sympathetic innervation and long-term left ventricular mechanical unloading. J Am Coll Cardiol Img 2010;3:64-70.
99. D'Orio Nishioka SA, Filho MM, Soares Brandão SC, Clementina Giorgi M, Vieira MLC, et al. Cardiac sympathetic activity pre and post resynchronization therapy evaluated by ^{123}I-MIBG myocardial scintigraphy. J Nucl Cardiol 2007;14:852-9.
100. Tomaselli GF, Zipes DP. What causes sudden death in heart failure? Circ Res 2004;95:754-63.
101. Moss AJ, Zareba W, Hall WJ, Klein H, Wilber DJ, Cannom DS, et al. Prophylactic implantation of a defibrillator in patients with myocardial infarction and reduced ejection fraction. N Engl J Med 2002;346:877-83.
102. Hohnloser SH, Connolly SJ, Kuck KH, Dorian P, Fain E, Hampton JR, et al. The defibrillator in acute myocardial infarction trial (DINAMIT): Study protocol. Am Heart J 2000;140:735-9.
103. Kadish A, Dyer A, Daubert JP, Quigg R, Estes NA, Anderson KP, et al. Prophylactic defibrillator implantation in patients with

nonischemic dilated cardiomyopathy. N Engl J Med 2004;350: 2151-8.
104. Fisher JD, Ector HE. Relative and absolute benefits: Main results should be reported in absolute terms. Pacing Clin Electrophysiol 2007;30:935-7.
105. Anderson KP. Estimates of implantable cardioverter-defibrillator complications: Caveat emptor. Circulation 2009;119:1069-71.
106. Anderson KP. Risk assessment for defibrillator therapy: II Trittico. J Am Coll Cardiol 2007;50:1158-60.
107. Lee DS, Krahn AD, Healey JS, Birnie D, Crystal E, Dorian P, et al. Evaluation of early complications related to De Novo cardioverter defibrillator implantation insights from the Ontario ICD database. J Am Coll Cardiol 2010;55:774-82.
108. Sanders GD, Hlatky MA, Owens DK. Cost-effectiveness of implantable cardioverter-defibrillators. N Engl J Med 2005;353: 1471-80.
109. Myerburg RJ. Implantable cardioverter-defibrillators after myocardial infarction. N Engl J Med 2008;359:2245-53.
110. Buxton AE, Lee KL, Hafley GE, Pires LA, Fisher JD, Gold MR, et al. Limitations of ejection fraction for prediction of sudden death risk in patients with coronary artery disease: Lessons from the MUSTT study. J Am Coll Cardiol 2007;50:1150-7.
111. de Vreede-Swagemakers JJ, Gorgels AP, Dubois-Arbouw WI, van Ree JW, Daemen MJ, Houben LG, et al. Out-of-hospital cardiac arrest in the 1990's: A population-based study in the Maastricht area on incidence, characteristics and survival. J Am Coll Cardiol 1997;30:1500-5.
112. Gorgels AP, Gijsbers C, de Vreede-Swagemakers J, Lousberg A, Wellens HJ. Out-of-hospital cardiac arrest-the relevance of heart failure. The Maastricht Circulatory Arrest Registry. Eur Heart J 2003;24:1204-9.
113. Stecker EC, Vickers C, Waltz J, Socoteanu C, John BT, Mariani R, et al. Population-based analysis of sudden cardiac death with and without left ventricular systolic dysfunction: Two-year findings from the Oregon Sudden Unexpected Death Study. J Am Coll Cardiol 2006;47:1161-6.
114. Al-Khatib SM, Hellkamp A, Curtis J, Mark D, Peterson E, Sanders GD, et al. Non-evidence-based ICD implantations in the United States. JAMA 2011;305:43-9.
115. Pertzov B NV, Zahger D, Katz A, Amit G. Insufficient compliance with current implantable cardioverter defibrillator (ICD) therapy guidelines in post myocardial infarction patients is associated with increased mortality. Int J Cardiol 2011. doi: 10.1016/j.ijcard.2011.10.132.
116. Krahn AD, Hoch JS, Rockx MA, Leong-Sit P, Gula LJ, Yee R, et al. Cost of preimplantation cardiac imaging in patients referred for a primary-prevention implantable cardioverter-defibrillator. Am J Cardiol 2008;102:588-92.
117. Passman R, Kadish A. Shouldn't everyone have an implantable cardioverter-defibrillator? Circulation 2009;120:2166-7.
118. Barron HV, Lesh MD. Autonomic nervous system and sudden cardiac death. J Am Coll Cardiol 1996;27:1053-60.
119. Gerson MC, Abdallah M, Muth JN, Costea AI. Will imaging assist in the selection of patients with heart failure for an ICD? JACC Cardiovasc Imaging 2010;3:101-10.
120. Arora R, Ferrick KJ, Nakata T, Kaplan RC, Rozengarten M, Latif F, et al. I-123 MIBG imaging and heart rate variability analysis to predict the needs for an implantable cardioverter defibrillator. J Nucl Cardiol 2003;10:121-31.
121. Nagahara D, Nakata T, Hashimoto A, Wakabayashi T, Kyuma M, Noda R, Shimoshige S, et al. Predicting the need for an implantable cardioverter defibrillator using cardiac metaiodobenzylguanidine activity together with plasma natriuretic peptide concentration or left ventricular function. J Nucl Med 2008;49:225-33.
122. Nishisato K, Hashimoto A, Nakata T, Doi T, Yamamoto H, Nagahara D, et al. Impaired cardiac sympathetic innervation and myocardial perfusion are related to lethal arrhythmia: Quantification of cardiac tracers in patients with ICDs. J Nucl Med 2010;51:1241-9.
123. Kasama S, Toyama T, Sumino H, Nakazawa M, Matsumoto N, Sato Y, et al. Prognostic value of serial cardiac ^{123}I-MIBG imaging in patients with stabilized chronic heart failure and reduced left ventricular ejection fraction. J Nucl Med 2008;49: 907-14.
124. Tamaki S, Yamada T, Okuyama Y, Morita T, Sanada S, Tsukamoto Y, et al. Cardiac iodine-123 Metaiodobenzylguanidine imaging predicts sudden cardiac death independently of left ventricular ejection fraction in patients with chronic heart failure and left ventricular systolic dysfunction: Results from a comparative study with signal-averaged electrocardiogram, heart rate variability, and QT dispersion. J Am Coll Cardiol 2009;53:426-35.
125. Senior R, Agostini D, Travin M, et al. Imaging of myocardial sympathetic innervation for prediction of arrhythmic events in heart failure patients: Insights from the ADMIRE-HF trial. Circulation 2009;120:S349 (abstract).
126. Boogers MJ, Borleffs CJ, Henneman MM, van Bommel RJ, van Ramshorst J, van Boersma E, et al. Cardiac sympathetic denervation assessed with 123-Iodine metaiodobenzylguanidine imaging predicts ventricular arrhythmias in implantable cardioverter-defibrillator patients. J Am Coll Cardiol 2010;55:2769-77.
127. Perrone-Filardi P, Paolillo S, Dellegrottaglie S, Gargiulo P, Savarese G, Marciano C, et al. Assessment of cardiac sympathetic activity by MIBG imaging in patients with heart failure: A clinical appraisal. Heart 2011;97:1828-33.
128. Mitrani RD, Klein LS, Miles WM, Hackett FK, Burt RW, Wellman HN, et al. Regional cardiac sympathetic denervation in patients with ventricular tachycardia in the absence of coronary artery disease. J Am Coll Cardiol 1993;22:1344-53.
129. Gill JS, Hunter GJ, Gane J, Ward DE, Camm AJ. Asymmetry of cardiac [^{123}I] meta-iodobenzylguanidine scans in patients with ventricular tachycardia and a ''clinically normal'' heart. Br Heart J 1993;69:6-13.
130. Schäfers M, Lerch H, Wichter T, Rhodes CG, Lammertsma AA, Borggrefe M, Hermansen F, et al. Cardiac sympathetic innervation in patients with idiopathic right ventricular outflow tract tachycardia. J Am Coll Cardiol 1998;32:181-6.
131. Wichter T, Matheja P, Eckardt L, Kies P, Schäfers K, Schulze-Bahr E, et al. Cardiac autonomic dysfunction in Brugada syndrome. Circulation 2002;105:702-6.
132. Miranda CH, Figueiredo AB, Maciel BC, Marin-Neto JA, Simões MV. Sustained ventricular tachycardia is associated with regional myocardial sympathetic denervation assessed with ^{123}I-metaiodobenzylguandine in chronic Chagas cardiomyopathy. J Nucl Med 2011;52:504-10.
133. Matsunari I, Schricke U, Bengel FM, Haase HU, Barthel P, Schmidt G, et al. Extent of cardiac sympathetic neuronal damage is determined by the area of ischemia in patients with acute coronary syndromes. Circulation 2000;101:2579-85.
134. Bengel FM, Barthel P, Matsunari I, Schmidt G, Schwaiger M. Kinetics of 123I-MIBG after acute myocardial infarction and reperfusion therapy. J Nucl Med 1999;40:904-10.
135. Henneman MM, Bengel FM, Bax JJ. Will innervation imaging predict ventricular arrhythmias in ischaemic cardiomyopathy? Eur J Nucl Med Mol Imaging 2006;33:862-5.

136. Inoue H, Zipes DP. Results of sympathetic denervation in the canine heart: Supersensitivity that may be arrhythmogenic. Circulation 1987;75:877-87.
137. Kammerling JJ, Green FJ, Watanabe AM, Inoue H, Barber MJ, Henry DP, et al. Denervation supersensitivity of refractoriness in noninfarcted areas apical to transmural myocardial infarction. Circulation 1987;76:383-93.
138. McGhie AI, Corbett JR, Akers MS, Kulkarni P, Sills MN, Kremers M, et al. Regional cardiac adrenergic function using I-123 Meta-Iodobenzylguanidine tomographic imaging after acute myocardial infarction. Am J Cardiol 1991;67:236-42.
139. Stanton MS, Tuli MM, Radtke NL, Heger JJ, Miles WM, Mock BH, et al. Regional sympathetic denervation after myocardial infarction in humans detected noninvasively using I-123-metaiodobenzylguanidine. J Am Coll Cardiol 1989;14:1519-26.
140. Sasano T, Abraham R, Chang KC, Ashikaga H, Mills KJ, Holt DP, et al. Abnormal sympathetic innervation of viable myocardium and the substrate of ventricular tachycardia after myocardial infarction. J Am Coll Cardiol 2008;51:2266-75.
141. Tomoda H, Yoshioka K, Shiina Y, Tagawa R, Ide M, Suzki Y. Regional sympathetic denervation detected by iodine 123 metaiodobenzylguanidine in non-Q-wave myocardial infarction and unstable angina. Am Heart J 1994;128:452-8.
142. Nakata T, Nagao K, Tsuchihashi K, Hashimoto A, Tanaka S, Iimura O. Regional cardiac sympathetic nerve dysfunction and diagnostic efficacy of metaiodobenzylguanidine tomography in stable coronary artery disease. Am J Cardiol 1996;78:292-7.
143. Inobe Y, Kugiyama K, Miyagi H, Ohgushi M, Tomiguchi S, Takahashi M, et al. Long-lasting abnormalities in cardiac sympathetic nervous system in patients with coronary spastic angina: Quantitative analysis with iodine 123 metaiodobenzylguanidine myocardial scintigraphy. Am Heart J 1997;134:112-8.
144. Watanabe K, Takahashi T, Miyajima S, Hirokawa Y, Tanabe N, Kato K, et al. Myocardial sympathetic denervation, fatty acid metabolism, and left ventricular wall motion in vasospastic angina. J Nucl Med 2002;43:1476-81.
145. Simula S, Vanninen E, Viitanen L, Kareinen A, Lehto S, Pajunen P, et al. Cardiac adrenergic innervation is affected in asymptomatic subjects with very early stage of coronary disease. J Nucl Med 2002;43:1-7.
146. Sakata K, Mochizuki M, Yoshida H, Nawada R, Ohbayashi K, Ishikawa J, et al. Cardiac sympathetic dysfunction contributes to left ventricular remodeling after acute myocardial infarction. Eur J Nucl Med 2000;27:1641-9.
147. Luisi AJ Jr, Fallavollita JA, Suzuki G, Canty JM Jr. Spatial inhomogeneity of sympathetic nerve function in hibernating myocardium. Circulation 2002;106:779-81.
148. Luisi AJ Jr, Suzuki G, Dekemp R, Haka MS, Toorongian SA, Canty JM Jr, et al. Regional 11C-hydroxyephedrine retention in hibernating myocardium: Chronic inhomogeneity of sympathetic innervation in the absence of infarction. J Nucl Med 2005;46:1368-74.
149. Canty JM Jr, Suzuki G, Banas MD, Verheyen F, Borgers M, Fallavollita JA. Hibernating myocardium: Chronically adapted to ischemia but vulnerable to sudden death. Circ Res 2004;94:1142-9.
150. Fallavollita JA, Canty JM Jr. Differential 18F-2-Deoxyglucose uptake in viable dysfunctional myocardium with normal resting perfusion: Evidence for chronic stunning in pigs. Circulation 1999;99:2798-805.
151. Hartikainen J, Mustonen J, Kuikka J, Vanninen E, Kettunen R. Cardiac sympathetic denervation in patients with coronary artery disease without previous myocardial infarction. Am J Cardiol 1997;80:273-7.
152. Fallavollita JA, Luisi AJ Jr, Michalek SM, Valverde AM, deKemp RA, Haka MS, et al. Prediction of arrhythmic events with positron emission tomography: PAREPET study design and methods. Contemp Clin Trials 2006;27:374-88.
153. Fallavollita JA, Canty JM Jr. Dysinnervated but viable myocardium in ischemic heart disease. J Nucl Cardiol 2010;17:1107-15.
154. Fallavollita J, Brendan M, Heavey BM, Baldwa S, Mashtare TL, Hutson AD, et al. Volume of denervated myocardium is a novel predictor of VT/VF: Prediction of Arrhythmic Events with Positron Emission Tomography (PAREPET) Study. http://www.abstractsonline.com/Plan/ViewAbstract.aspx?sKey=6c291506-005d-4285-a1ce-2200099a765d&cKey=b896d37f-5743-4eb0-9a43-0904dd8d6f31&mKey=%7bBAEF2DB4-7615-4F2C-851A-E5D7461EBD4E%7d. Accessed 9/24/2012.
155. Akutsu Y, Kaneko K, Kodama Y, Li HL, Suyama J, Shinozuka A, et al. Iodine-123 mIBG imaging for predicting the development of atrial fibrillation. J Am Coll Cardiol Imaging 2011;4:78-86.
156. Schwaiblmair M, von Scheidt W, Uberfuhr P, Ziegler S, Schwaiger M, Reichart B, et al. Functional significance of cardiac reinnervation in heart transplant recipients. J Heart Lung Transplant 1999;18:838-45.
157. Estorch M, Campreciós M, Flotats A, Marí C, Bernà L, Catafau A, et al. Sympathetic reinnervation of cardiac allografts evaluated by 123I-MIBG imaging. J Nucl Med 1999;40:911-6.
158. Hattori N, Tamaki N, Hayashi T, Masuda I, Kudoh T, Tateno M, et al. Regional abnormality of iodine-123-MIBG in diabetic hearts. J Nucl Med 1996;37:1985-90.
159. Langer A, Freeman MR, Josse RG, Armstrong PW. Metaiodobenzylguanidine imaging in diabetes mellitus assessment of cardiac sympathetic denervation and its relation to autonomic dysfunction and silent myocardial ischemia. J Am Coll Cardiol 1995;25:610-8.
160. Nagamachi S, Fujita S, Nishii R, Futami S, Tamura S, Mizuta M, et al. Prognostic value of cardiac I-123 metaiodobenzylguanidine imaging in patients with non-insulin-dependent diabetes mellitus. J Nucl Cardiol 2006;13:34-42.
161. Yufu K, Takahashi N, Okada N, Shinohara T, Nakagawa M, Hara M, et al. Cardiac iodine-123 metaiodobenzylguanidine (^{123}I-MIBG) scintigraphy parameter predicts cardiac and cerebrovascular events in type 2 diabetic patients without structural heart disease. Circ J 2012;76:399-404.
162. Valdés Olmos RA, ten Bokkel Huinink WW, ten Hoeve RF, van Tinteren H, Bruning PF, van Vlies B, et al. Assessment of anthracycline related myocardial adrenergic derangement by [123I]metaiodobenzylguanidine scintigraphy. Eur J Cancer 1995;31:26-31.
163. Carrió I, Estorch M, Berna L, López-Pousa J, Tabernero J, Torres G. Assessment of anthracycline-related myocardial adrenergic Indium-111-antimyosin and iodine-123-MIBG studies in early assessment of doxorubicin cardiotoxicity. J Nucl Med 1995;36:2044-9.